Feasibility of 18F-FDG Dose Reductions in Breast Cancer PET/MRI

Bert-Ram Sah[1,2,3,4], Soleen Ghafoor[3,4], Irene A. Burger[1,4,5], Edwin E.G.W. ter Voert[1,4],

Tetsuro Sekine[1], Gaspar Delso[1,6], Martin Huellner[1,4], Konstantin J. Dedes[5,7], Andreas

Boss[3,4], Patrick Veit-Haibach[1,3,4,8,9]

[1]   *Department of Nuclear Medicine, University Hospital of Zurich*

[2]   *Department of Cancer Imaging, King`s College London*

[3]   *Department of Diagnostic and Interventional Radiology, University Hospital of Zurich*

[4]   *University of Zurich*

[5]   *Cancer Center Zurich*

[6]   *GE Healthcare, Waukesha, WI, USA*

[7]   *Department of Gynaecology, University Hospital of Zurich*

[8]   *Joint Department Medical Imaging, University Health Network, Toronto, Ontario, Canada*

[9]   *University of Toronto, Toronto, Ontario, Canada*

University Hospital of Zurich: Raemistrasse 100, CH-8091 Zurich, Switzerland

Corresponding Author:

Bert-Ram Sah, MD

Department of Nuclear Medicine, Department of Diagnostic and Interventional Radiology

University Hospital of Zurich

Raemistrasse 100, CH-8091 Zurich

Tel. 0041 44 255 11 11, Fax. 0041 44 255 44 14

E-mail address: bert-ram.sah@usz.ch

Soleen Ghafoor: Soleen.Ghafoor@usz.ch

Irene A. Burger: Irene.Burger@usz.ch

Edwin E.G.W. ter Voert: Edwin.terVoert@usz.ch

Tetsuro Sekine: tetsuro.sekine@gmail.com

Gaspar Delso: GasparDelso@ge.com

Martin Huellner: Martin.Huellner@usz.ch

Konstantin J. Dedes: konstantin.dedes@usz.ch

Andreas Boss: Andreas.Boss@usz.ch

Patrick Veit-Haibach: Patrick.Veit-Haibach@uhn.ca

Running title: Dose Reduction in PET/MRI

ABSTRACT

Rationale The goal of this study was to determine the level of clinically acceptable 18F-fluoro-2-deoxy-D-glucose (18F-FDG) dose reduction in time of flight (TOF) - positron emission tomography/magnetic resonance imaging (PET/MRI) in patients with breast cancer.

Methods Twenty-six consecutive female patients with histologically proven breast cancer were analyzed (median age, 51 years; range, 34 – 83 years). Simulated dose-reduced PET images were generated by un-listing the list mode data on PET/MRI. The acquired 20 minutes PET frame was reconstructed in 5 ways: a reconstruction of the first 2 minutes with 3 iterations and 28 subsets for reference, and reconstructions simulating 100%, 20%, 10%, 5% of the original dose. General image quality and artifacts (GIQ+A), image sharpness (IS), noise, and lesion detectability (LD) were analyzed using a four-point scale. Qualitative parameters were compared by using the non-parametric Friedman test for multiple samples and the Wilcoxon signed-rank test for paired samples. Comparison of different groups of independent samples was performed using the Mann-Whitney-U-Test.

Results Overall, 355 lesions (71 lesions with five different reconstructions each) were evaluted. The 20 minutes reconstruction with 100% injected dose showed the best results in all categories. In GIQ+A, IS and noise the reconstructions with a simulated dose of 20% and 10% were significantly better than the 2 minutes reconstructions ($p<=0.001$). Furthermore, 20%, 10%, and 5% reconstructions did not yield different results compared to the 2 minutes reconstruction in LD of the primary lesion. Using 10% of the injected dose a calculated mean dose of 22.6 +/- 5.5 MBq (range 17.9 – 36.9

MBq) would have been applied, resulting in an estimated whole-body radiation burden of 0.5 +/- 0.1 mSv (range 0.4 – 0.7 mSv).

Conclusion 10% of the standard dose of 18F-FDG (reduction of up to 90%) results in clinically acceptable PET-image quality in TOF PET/MRI. The calculated radiation exposure would be comparable to the effective dose of a single digital mammography. A reduction of radiation burden to this level might justify partial-body examinations with PET/MRI for dedicated indications.

Key Words

Dose reduction, Positron Emission Tomography, Magnetic Resonance, image reconstruction, breast cancer

Word Count (Introduction through Discussion): 3698.

INTRODUCTION

Positron emission tomography/computed tomography (PET/CT) is one of the most widely used hybrid imaging tools for staging, therapy response assessment and follow-up of different malignant diseases (1,2). In PET/CT, the CT-component is used for attenuation correction as well as for anatomical correlation and characterization of neoplastic lesions, while the PET-component is used to identify lesions with increased radiotracer uptake (3,4). In breast cancer, clinical PET/CT has been mainly used as whole-body examination for detection, therapy follow up and response assessment, as well as prognostic stratification (5). Despite promising results with PET-mammography (PEM), conventional mammography, ultrasound and magnetic-resonance imaging (MRI) are the predominant diagnostic imaging tools for local staging (6-8).

Since several years, PET/MRI has been used clinically and scientifically for the evaluation of a number of neoplastic diseases (9,10). In such systems, the MRI component replaces the CT-component for attenuation correction and anatomical reference. Since the MRI-component is known to have a much higher soft tissue contrast and because MRI can provide additional information (e.g. diffusivity, intravoxel incoherent motion, iron load, blood oxygenation level dependent effect, etc.) it is expected to have an even greater impact on diagnostic and therapeutic decisions in certain oncological patients than PET/CT – which remains yet to be proven (9,11-14).

In breast cancer, MRI is mainly used for detection, characterization, biopsy guidance of lesions, but also partially for screening (15). Nonetheless, as every imaging modality, the MRI has its technically inherent limitations. Alternatively, PEM has already been proven to be helpful in characterizing small breast lesions (16). However PEM

scanners are very specialized systems that cannot be used for a broader range of imaging, and they are not widely available yet. Another argument PET-imaging is constantly confronted with is the radiation exposure to the patient, especially in breast imaging.

New PET technologies used in PET/MRI were shown to reduce the radiation burden significantly (17), and the PET component from the latest clinical TOF-PET/MRI system has the potential to reduce radiation exposure even further, especially in single-station imaging. This system uses a new PET detector based on silicon photomultipliers (SiPM), that offers increased sensitivity compared to conventional PET/CT and PET/MRI scanner. This allows the user to balance dose reduction with acquisition time (18).

In our study, we evaluated and compared the overall image quality, artifacts, image sharpness, noise, and lesion detectability of breast cancer in PET/MRI-images with simulated, reduced 18F-FDG doses. We used a 2 minute (per bed position) acquisition as a standard of reference, since this acquisition time is widely used in standard clinical care.

The goal of this study was to determine the acceptable level of 18F-FDG dose reduction in TOF-PET/MRI using a SiPM PET detector for breast cancer assessment.

MATERIALS AND METHODS

Ethics Approval and Consent to Participate

All procedures performed in studies involving human participants were in accordance with the ethical standards of the institutional and/or national research committee and with the 1964 Helsinki declaration and its later amendments or comparable ethical standards. The institutional review board approved this study. Patients were acquired prospectively as part of a larger study with several different subgroups (KEK-ZH Nr. 2014-0072 / NCT02316431). All patients gave written informed consent prior to inclusion into the study. There was financial support for this study from GE Healthcare on an institutional level. GE-Healthcare employed personnel participated in this study as authors. Only non-GE Healthcare employees had control of inclusion of the data and information that might present a conflict of interest.

Patients

Patients had to meet the following criteria for inclusion in our study: referral for a clinical (based on local clinical guidelines) PET/CT for initial staging of a histologically confirmed breast cancer. Additionally, the patient needed to be willing to undergo the additional scientific PET/MRI examination of the breast. Exclusion criteria were contraindications to MRI imaging, such as electronically active implanted medical devices, metallic foreign bodies in sensitive anatomical areas (e.g. orbita), severe claustrophobia, or a body size that did not fit into the PET/MRI bore.

Imaging

Patients fasted at least 4 hours prior to injection of the tracer. Patients for clinical PET/CT were injected intravenously with 3 MBq of ^{18}F-FDG per kilogram of body weight for patients with body weight <= 85 kg and 3.5 MBq/kg otherwise. The PET/CT was acquired ca. 1 hour after tracer administration. Patients were only injected once with FDG for the clinical PET/CT, no additional injection was done for the PET/MRI. The uptake time for the 20 minute PET frame was 34 ± 6 min.

The PET/CT acquisition followed our standard protocol for clinical oncologic imaging on a TOF-PET/CT scanner as previously published (Discovery 690 TOF PET/CT, GE Healthcare, Waukesha, WI) (19,20). The PET/MR system is located in an adjacent room next to the PET/CT room, thus the time difference between the start of the acquisitions was 38 ± 3.5 min.

PET/MRI Acquisition. PET/MRI imaging was performed on a simultaneous time-of-flight (TOF) PET/MRI scanner (SIGNA PET/MR, GE Healthcare, Waukesha, WI, USA). Patients were positioned on an 8-channel breast coil (GE Healthcare, Waukesha, WI, USA) in prone position. The coil has a fixed position on the bed, allowing it to be automatically included in the PET attenuation correction.

The PET transaxial field-of-view (FOV) is 60cm and the axial FOV is 25cm; allowing the area of interest to be scanned within a single PET bed position (21). The per crystal TOF timing resolution is < 400ps (22), enabling TOF imaging. PET list mode data was acquired in 3 dimensional (3D) TOF mode with a scan duration of 20 minutes in the breast-bed position. An axial FOV of 25cm was used. The scan time for the PET was adapted based on the MRI-protocol needed for a dedicated breast MRI-examination.

During PET/MRI scanning a default (DIXON based) MRI acquisition for attenuation correction was performed. Additionally, a dedicated breast MRI-protocol was acquired for diagnostic purposes (for technical details, see Supplemental Table 1).

Image Processing. For each patient, the 20 minutes PET frame was reconstructed in 5 different sets: a reconstruction of the first 2 minutes with 3 iterations and 28 subsets for reference and comparison (2min), followed by reconstructions simulating 100% (100% of injected 18F-FDG dose), 20%, 10%, 5% of the original dose (injected for the clinical PET/CT), all with 20 minutes acquisition time. These percentages were selected based on a pre-evaluation in which image quality parameters on higher percentages did not show significant differences compared to the standard-of-reference. The 100% and 20% datasets were reconstructed with 3 iterations and 28 subsets, the 10% and 5% datasets with 50 iterations and 1 subset. The different reconstructions were chosen to reflect the differences in counts per reconstruction (the lower the counts, the lower the number of subsets has to be in order to avoid excessive noise).

Reduction of injected 18F-FDG was simulated by removing the required amount of counts from the list-mode data. This was performed randomly on a microsecond by microsecond basis (with an in-house MatLab script).

This way, the total scan time remains 20 minutes and, as a result, the data still includes normal effects such as decay, biodistribution and eventual patient motion. The PET images were reconstructed using the system's default 3D ordered subsets expectation maximization iterative reconstruction algorithm which includes all default corrections and incorporates TOF information. The image grid was 256x256 pixels and images were filtered in image space using a 4-mm full width at half maximum in-plane

Gaussian filter followed by an axial filter with a 3-slice kernel using relative weights of 1:4:1.

Image Evaluation. A total of 130 reconstructed PET data sets (26 patient studies with 5 different reconstructions each, see above) were evaluated in consensus by two experienced nuclear medicine physicians/radiologists (with 5 and 6 years of experience interpreting PET and MRI, respectively). These readers were aware of the clinical background of the study, but blinded to the reconstruction method used. For further analysis, lesions were grouped according to their location (primary breast lesions, lymph nodes and distant metastases). Lesions were selected independently of their size. If more than one lesion was present, target lesions were randomly defined for further analysis, covering a range of sizes. Per patient, all suspicious PET-positive primary lesions (n = 1 to 3 lesions per patient) and lymph nodes (n = 0 to 4), and a maximum of four suspicious PET-positive lesions in the lung (n = 0 to 4) and/or bone (n = 0 to 2) were chosen. A suspicious abdominal lesion was present in only one patient. If more than one suspicious lesion was present in the lung or bone, target lesions were defined for further analysis, covering a range of sizes and subsegments of the compartments (e.g. different lung segments or bones). Size and Maximum Standardized Uptake Value of lesions were measured. The size was measured in a post-contrast T1-weighted 3D fast spoiled gradient echo acquisition. Image evaluation was done using the "COMPARE" protocol of an AW Workstation Version 4.5 (GE Healthcare Biosciences, Pittsburgh, USA) (23). The two-reader setup was chosen to prove reliability of semi-quantitative image analyses(24). For the respective analysis, PET-data sets were viewed in all three planes. The two readers subjectively evaluated general image quality

and artifacts (GIQ+A), image sharpness (IS), noise and lesion detectability (LD) using a four-point scale (Table 1) (24).

Statistical Analysis

Continuous variables were expressed as means +/- standard deviations and categorical variables such as qualitative parameters as frequencies (percentages). For the primary lesions, the median "size" was calculated (which was 1.7 cm). Lesions were subsequently defined as "small" when smaller than the median size of 1.7 cm and "large" when larger than 1.7 cm. Comparison of different groups of independent samples (lesion size) was performed using the Mann-Whitney-U-Test. Regarding qualitative parameters, we compared the five reconstructions with respect to GIQ+A, IS, noise and LD using the non-parametric Friedman test for multiple samples and the Wilcoxon signed-ranks test for paired samples.

Data analysis was performed using commercially available software (SPSS Statistics 21, release 21.0.0, IBM, Chicago, IL, USA). A p-value < 0.05 indicates statistical significance.

RESULTS

Overall, 26 consecutive female patients with histologically proven breast cancer were analyzed (median age, 51 years; range, 34 – 83 years). Patients had invasive breast cancer of no special type (n = 19), invasive lobular breast cancer (n = 3), metaplastic breast cancer (n = 2), tubular breast cancer (n = 1), or cirbiform breast cancer (n = 1). Altogether, 355 lesions (71 lesions with five different reconstructions) were eveluted.

There were 36 (51%) primary breast lesions, 26 axillary, hilar or internal mammary chain lymph nodes (37%) and 9 (13%) bone, lung or abdominal lesions. Oestrogen receptor alpha was positive in 13 (50%), progesterone receptor in 16 (62%), and the human epidermal growth factor receptor 2 in 9 of 26 (35%) patients. Staging of patients is shown in Supplemental Table 2.

Image Quality and Artifacts

Rating of GIQ+A showed significant differences between several reconstructions (p<0.001, Friedman). GIQ+A was rated best in the 20min reconstruction with 100% dose (Table 2 for mean rating, Table 3 for comparison). Reconstructions with reduction of dose down to 20% and 10% showed significantly better results than the 2min reconstruction, and the reconstruction with 5% dose of injected tracer was not rated significantly different than the 2min scan.

Image sharpness

Similar, rating of IS showed significant differences between reconstructions (p<0.001, Friedman). IS was rated best in the 20min reconstruction with 100% dose (Table 2 for

mean rating, Table 3 for comparison). Reconstructions with reduction of dose to 20% and 10% showed significantly better results than the 2min reconstruction, and the reconstruction with 5% dose of injected tracer was rated significantly inferior to the 2min scan.

Noise

Finally, also rating of noise showed significant differences between reconstructions ($p<0.001$, Friedman). Noise was rated best in the 20min reconstruction with 100% dose (Table 2 for mean rating, Table 3 for comparison). Reconstructions with reduction of dose down to 20% and 10% showed significantly better results than the 2min reconstruction, and the reconstruction with 5% dose of injected tracer was not rated significantly different than the 2min scan.

Lesion Detectability

LD was rated to be good to excellent in all reconstructions. Best results were obtained with the 20min 100% reconstruction, significantly better than in the 2min reconstruction (for primary lesions). 20% and 10% reconstructions were rated better than the 2min reconstruction, without significant differences in primary lesions. The 5% reconstruction was rated inferior compared to the 2min reconstruction, however without significant differences in primary lesions or lymph nodes.

Lesion Size

Primary lesions (mean: 2.0 +/- 1.0cm, range: 0.9 – 4.3cm, median 1.7cm) were grouped into small lesions (<1.7cm) and large lesions (>1.7cm). The first group includes also eight lesions < 1cm. There was no significant difference in rating between small and

large lesions (p=0.538 for the 2min reconstruction, p=0.599 for 20min 100%, p=0.753 for 20min 20%, p=1.0 for 20min 10%, and p=0.461 for the 20min 5% reconstruction, respectively).

Calculation of Radiation Burden

Patients were injected 225.8 +/- 55 MBq of ^{18}F-FDG (range 179 – 369 MBq), resulting in an estimated whole-body radiation burden of 4.5 +/- 1.1 mSv (range 3.6 – 7.3 mSv) (25).

Using 20% of the injected dose a calculated mean dose of 45.2 +/- 11.0 MBq (range 35.8 – 73.6 MBq) would have been applied, resulting in an estimated whole-body radiation burden of 0.9 +/- 0.2 mSv (range 0.7 – 1.5 mSv). Similarly, using 10% of the injected dose a calculated mean dose of 22.6 +/- 5.5 MBq (range 17.9 – 36.9 MBq) would have been applied, resulting in an estimated whole-body radiation burden of 0.5 +/- 0.1 mSv (range 0.4 – 0.7 mSv). Or, using 5% of the injected dose a calculated mean dose of 11.3 +/- 2.8 MBq (range 9 – 18.5 MBq) would have been applied, resulting in an estimated whole-body radiation burden of 0.2 +/- 0.1 mSv (range 0.2 – 0.4 mSv).

DISCUSSION

Our study showed that a dose reduction of up to 90% on a state-of-the-art TOF-PET/MRI system with SiPM detectors for single station imaging is feasible with clinically acceptable image quality.

The overall image quality in the reconstructions with a simulated dose of only 10% of the standard dose was found adequate in all measured categories, translating into a reduction of up to 90% of the injected 18F-FDG-dose. The image quality with 5% of the standard dose (reduction of up to 95%) was comparable to the currently clinically used 2 min scan. However it was rated to have significantly inferior image sharpness. Compared to the currently clinically used 2 min scan, the lesion detectability was not impaired when the dose was reduced to 5% of the clinically injected 18F-FDG-dose. These results indicate the possiblity of a significant dose reduction in PET/MRI of suspicious breast lesions. A reduction of 90% would result in an estimated effective dose of approximately 0.45 mSv for a patient weighting 75 kg (3 MBq/kg x 10/100 x 75 kg x 0.0199 mSv/MBq) (25). For comparison - the average effective dose for mammography - which is a widely used imaging modality for breast cancer screening ranges from 0.44 mSv – 0.56 mSv (26). This comparison is not entirely adequate, since the radiation burden in PET/MRI accounts for the whole body, while in mammography it is focused on a single anatomic area and the radiation burden to other organs is below 1% of the focused radiation (27). However, other advantages are associated with lower activities which are not picked by the under-sampling technique e.g. the randoms rate would be a lower proportion of the total count rate at reduced activities.

Our results show the advantage of the new technology used. Attributed to the new solid-state detector design, increased axial FOV and Compton scatter recovery, a significantly increased sensitivity is provided, which in turn may compensate for the here described dose reduction (28). Our results are also in line with the data of Seit et al., who investigated the effect of dose reduction in whole body PET examinations on a PET/MRI scanner without TOF capability and lutetium oxyorthosilicate detector crystals. It was concluded that a reduction of 18F-FDG of up to 33% was feasible (29) (dose reduction to 2 MBq/kg BW (Biograph Siemens PET MRI)). In a previous study by our group, we showed that using a TOF-capable PET-component, a dose reduction of up to 50% was feasible in whole body acquisitions in patients with normal body weight (17).

In the herewith presented study we were able to show that in single-station imaging (lesions in the breast and axilla), the injected dose could be reduced even more than in whole-body PET scans. The main reason for this reduction is obviously the imaging/acquisition time for this specific bed position which is bound to the imaging times needed for MR-mammography (or any other MR-imaging). Imaging times for MR-mammography in the literature range from as short as 12 minutes up to > 20 minutes. When PET detectors are kept listening throughout the entire MR mammography, significantly more counts are received compared to standard whole-body imaging (usually 2-4 minutes/bed position). This in turn opens the opportunity to balance acquisition time versus injected dose. Another reason for the significant reduction is also that suspicious lesions in the breast or axillary lymph node region are relatively superficial and that they are usually surrounded by fatty tissue or glandular breast tissue, which results in a high signal-to-noise ratio. We suppose that results might be somewhat less impressive e.g. in single-station liver imaging, where a high background noise is

16

present. As shown in a study by Gatidis et al., clinical evaluation of image quality is in line with quantitative image metrics, and that retrospective under-sampling of list mode data results in equivalent image properties compared to PET images measured at low doses (30).

To date, PET imaging in oncologic examinations is mainly restricted to whole-body examinations in patients with different cancer indications. This was somewhat justified by the radiation burden in the current clinical setting (5-15 mSv for a PET/CT). With the results of this study, this restriction might potentially be reconsidered. Having the possibility to reduce the amount of injected tracer for specific indications will significantly reduce the radiation burden of patients – which may result in a paradigm shift in PET-imaging. A reduction of injected dose as presented in our results will render partial-body examinations with PET/MRI justifiable. Reduction of PET-induced radiation exposure may not only reduce possible radiation-related risks, but may also improve acceptance of PET among patients and referring physicians (30). By opening up the PET/MRI to more indications than currently, PET/MRI might even become possibly more economically viable (a certainly welcome side effect). One specific example could possibly be the work-up of Breast Imaging Reporting and Data System 3 lesions. These lesions cannot be sufficiently classified and therefore usually need follow-up. Work-up of such lesions with a rather low probability of malignancy requires techniques with low (or none) radiation exposure, in order to have an acceptable risk-benefit-ratio. MRI is partly used for this indication, but has certain limitations. Also, they may occur in younger patients, who are at higher risk for developing radiation-induced diseases. PET/MRI has the potential for multiparametric qualitative and quantitative feature characterization and

therefore can improve tumor characterization and outcome prediction (31). Also, it has already been shown that it is useful in whole-body staging of patients with invasive ductal breast carcinoma and recurrent breast cancer (11,14,32). The potential to characterize breast lesions with PET-techniques with high accuracy has been demonstrated by Yamamoto et al. In a screening setting with 265 women they were able to show, that abnormal FDG-uptake (detected with PEM) showed a sensitivity of 100% and a specificity of 84.5%. In their study, PET-imaging showed a detection rate of 2.3%, which is higher than the reported detection rate of mammography and physical examination (0.31%), but may be partly explained by a selection bias in their study (16). The authors concluded that the detection of an abnormal 18F-FDG uptake had potential for breast cancer screening. PEM offers the possibility for better image quality of breast lesions, since the detectors are closer to the lesion, which results in a higher spatial resolution. However, there is no study comparing the sensitivity of PEM to newly available PET systems with SiPM detectors, which have a very high sensitivity, but are obviously not as close to the breast tissue as within a PEM-system. PEM systems are not widely available and still fail to be considered a useful adjunct to MRI in clinical imaging, despite very promising initial results (16,33,34).

It should be noted that the results of our study are not necessarily restricted to imaging with 18F-FDG. Currently, there are several receptor specific tracers under investigation, which offer potential beyond the means of current clinical imaging. These are, for example, 18F-FES, a fluorinated estradiol, targeting the estrogen receptor, radionuclides targeting the human epidermal growth factor receptor 2, Somatostatin receptor mediated imaging, or gastrin-releasing peptide receptor imaging, which could

be applied for disease characterisation, staging or monitoring therapy response (35). However, those research questions have to be investigated separately.

We would like to outline that our study has several limitations. The results of our study are limited to the breast and axillary region. Those regions offer a higher signal-to-noise ratio, since there is a lot of low FDG-avid adipose tissue. Other indications, for example assessment of suspicious liver lesions should be investigated in further studies. In the present study, only 3 of our 26 patients (12%) had a body mass index above 30. In obese patients higher injected doses are expected for adequate image quality. We included only patients with biopsy-proven breast cancer lesions, who underwent whole-body PET/CT. Therefore and because there is a certain patient selection bias in our population towards more aggressive breast cancer types, our study does not allow to draw a conclusion, to which extent the uptake of 18F-FDG might contribute to the diagnostic work-up of suspicious (but not yet proven malignant) breast lesions. However, this has been addressed in several previous studies with promising results (34).

CONCLUSION

PET-detectors with SiPM and TOF capability offer a high quality in single-station PET/MRI imaging. A dose reduction of up to 90% of currently clinically used injected dose of 18F- FDG was found to be adequate for single-station breast imaging. The calculated radiation exposure would be comparable to the effective dose of a single digital mammography. A reduction of radiation burden to this level will possibly render partial-body examinations with PET/MRI justifiable.

DECLARATIONS

REFERENCES

1. Hess S, Blomberg BA, Zhu HJ, Hoilund-Carlsen PF, Alavi A. The pivotal role of FDG-PET/CT in modern medicine. *Acad Radiol.* 2014;21:232-249.

2. Sheikhbahaei S, Mena E, Pattanayak P, Taghipour M, Solnes LB, Subramaniam RM. Molecular imaging and precision medicine: PET/computed tomography and therapy response assessment in oncology. *PET Clin.* 2017;12:105-118.

3. Townsend DW. Dual-modality imaging: combining anatomy and function. *J Nucl Med.* 2008;49:938-955.

4. Muzic RF, Jr., DiFilippo FP. Positron emission tomography-magnetic resonance imaging: technical review. *Semin Roentgenol.* 2014;49:242-254.

5. Kiser J. Molecular imaging and its role in the management of breast cancer. *Clin Obstet Gynecol.* 2016;59:403-411.

6. Giess CS, Chikarmane SA, Sippo DA, Birdwell RL. Breast MR imaging for equivocal mammographic findings: help or hindrance? *Radiographics.* 2016;36:943-956.

7. Bychkovsky BL, Lin NU. Imaging in the evaluation and follow-up of early and advanced breast cancer: When, why, and how often? *Breast.* 2017;31:318-324.

8. Berg WA. Nuclear breast imaging: Clinical results and future directions. *J Nucl Med.* 2016;57 Suppl 1:46S-52S.

9. Melsaether A, Moy L. Breast PET/MR imaging. *Radiol Clin North Am.* 2017;55:579-589.

10.   Rice SL, Friedman KP. Clinical PET-MR imaging in breast cancer and lung cancer. *PET Clin.* 2016;11:387-402.

11.   Sawicki LM, Grueneisen J, Schaarschmidt BM et al. Evaluation of (1)(8)F-FDG PET/MRI, (1)(8)F-FDG PET/CT, MRI, and CT in whole-body staging of recurrent breast cancer. *Eur J Radiol.* 2016;85:459-465.

12.   Gillies RJ, Beyer T. PET and MRI: Is the whole greater than the sum of its parts? *Cancer Res.* 2016;76:6163-6166.

13.   Melsaether AN, Raad RA, Pujara AC et al. Comparison of whole-body (18)F FDG PET/MR imaging and whole-body (18)F FDG PET/CT in terms of lesion detection and radiation dose in patients with breast cancer. *Radiology.* 2016;281:193-202.

14.   Grueneisen J, Sawicki LM, Wetter A et al. Evaluation of PET and MR datasets in integrated 18F-FDG PET/MRI: A comparison of different MR sequences for whole-body restaging of breast cancer patients. *Eur J Radiol.* 2017;89:14-19.

15.   Kuhl CK. The changing world of breast cancer: A radiologist's perspective. *Plast Surg Nurs.* 2016;36:31-49.

16.   Yamamoto Y, Tasaki Y, Kuwada Y, Ozawa Y, Inoue T. A preliminary report of breast cancer screening by positron emission mammography. *Ann Nucl Med.* 2016;30:130-137.

17.   Sekine T, Delso G, Zeimpekis KG et al. Reduction of 18F-FDG dose in clinical PET/MR imaging by using silicon photomultiplier detectors. *Radiology.* 2017:162305.

18. Herzog H, Lerche C. Advances in clinical PET/MRI instrumentation. *PET Clin.* 2016;11:95-103.

19. Queiroz MA, Delso G, Wollenweber S et al. Dose optimization in TOF-PET/MR compared to TOF-PET/CT. *PLoS One.* 2015;10:e0128842.

20. Zeimpekis KG, Barbosa F, Hullner M et al. Clinical evaluation of PET image quality as a function of acquisition time in a new TOF-PET/MRI compared to TOF-PET/CT--Initial results. *Mol Imaging Biol.* 2015;17:735-744.

21. Ter Voert E, Delso G, de Galiza Barbosa F, Huellner M, Veit-Haibach P. The effect of defective PET detectors in clinical simultaneous [(18)F]FDG time-of-flight PET/MR imaging. *Mol Imaging Biol.* 2017;19:626-635.

22. Levin C GG, Deller T, McDaniel DL, Peterson W, Maramraju SH. Prototype time-of-flight PET ring integrated with a 3T MRI system for simultaneous whole-body PET/MR imaging. *Society of Nuclear Medicine Annual Meeting Abstracts.* 2013;54.

23. Sah BR, Stolzmann P, Delso G et al. Clinical evaluation of a block sequential regularized expectation maximization reconstruction algorithm in 18F-FDG PET/CT studies. *Nucl Med Commun.* 2017;38:57-66.

24. Stansfield EC, Sheehy N, Zurakowski D, Vija AH, Fahey FH, Treves ST. Pediatric 99mTc-MDP bone SPECT with ordered subset expectation maximization iterative reconstruction with isotropic 3D resolution recovery. *Radiology.* 2010;257:793-801.

25.   Quinn B, Dauer Z, Pandit-Taskar N, Schoder H, Dauer LT. Radiation dosimetry of 18F-FDG PET/CT: incorporating exam-specific parameters in dose estimates. *BMC Med Imaging.* 2016;16:41.

26.   Hendrick RE. Radiation doses and cancer risks from breast imaging studies. *Radiology.* 2010;257:246-253.

27.   Sechopoulos I, Suryanarayanan S, Vedantham S, D'Orsi CJ, Karellas A. Radiation dose to organs and tissues from mammography: Monte Carlo and phantom study. *Radiology.* 2008;246:434-443.

28.   Grant AM, Deller TW, Khalighi MM, Maramraju SH, Delso G, Levin CS. NEMA NU 2-2012 performance studies for the SiPM-based ToF-PET component of the GE SIGNA PET/MR system. *Med Phys.* 2016;43:2334.

29.   Seith F, Schmidt H, Kunz J et al. Simulation of tracer dose reduction in (18)F-FDG PET/MRI: Effects on oncologic reading, image quality, and artifacts. *J Nucl Med.* 2017;58:1699-1705.

30.   Gatidis S, Wurslin C, Seith F et al. Towards tracer dose reduction in PET studies: Simulation of dose reduction by retrospective randomized undersampling of list-mode data. *Hell J Nucl Med.* 2016;19:15-18.

31.   Plecha DM, Faulhaber P. PET/MRI of the breast. *Eur J Radiol.* 2017;94:A26-A34.

32.   Catalano OA, Daye D, Signore A et al. Staging performance of whole-body DWI, PET/CT and PET/MRI in invasive ductal carcinoma of the breast. *Int J Oncol.* 2017;51:281-288.

33.   Tafra L, Cheng Z, Uddo J et al. Pilot clinical trial of 18F-fluorodeoxyglucose
       positron-emission mammography in the surgical management of breast cancer.
       Am J Surg. 2005;190:628-632.

34.   Bitencourt AG, Lima EN, Macedo BR, Conrado JL, Marques EF, Chojniak R. Can
       positron emission mammography help to identify clinically significant breast
       cancer in women with suspicious calcifications on mammography? *Eur Radiol.*
       2017;27:1893-1900.

35.   Dalm SU, Verzijlbergen JF, De Jong M. Review: Receptor targeted nuclear
       imaging of breast cancer. *Int J Mol Sci.* 2017;18.
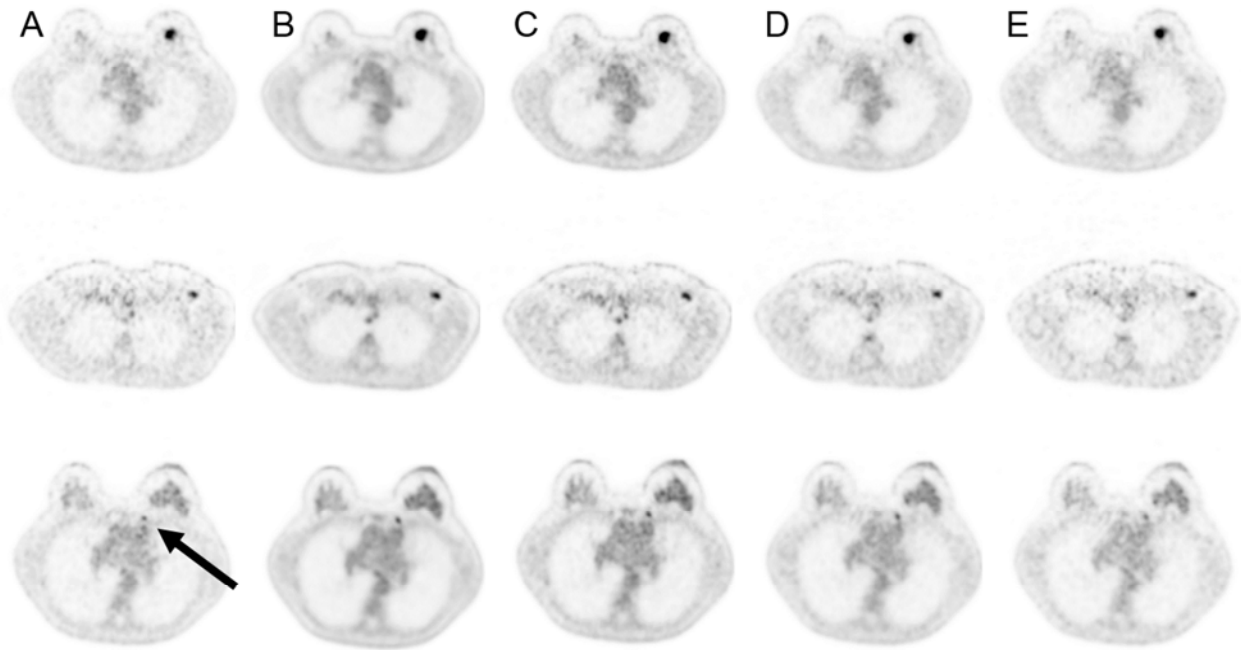
FIGURE LEGEND

Figure 1. 57 year old patient with invasive left sided breast cancer (1st row), an axillary lymph node metastasis (2nd row) and an internal mammary lymph node (3rd row). The patient was injected with 180 MBq of FDG (body weight of 60 kg).

A: 2 min TOF, B: 100% of FDG dose, C: 36 MBq FDG (20% dose), D: 18 MBq FDG (10% dose), E: 9 MBq FDG (5% dose). For a PET/MRI examination with the images shown in column D, this patient would receive an estimated radiation burden of 0.36 mSv.
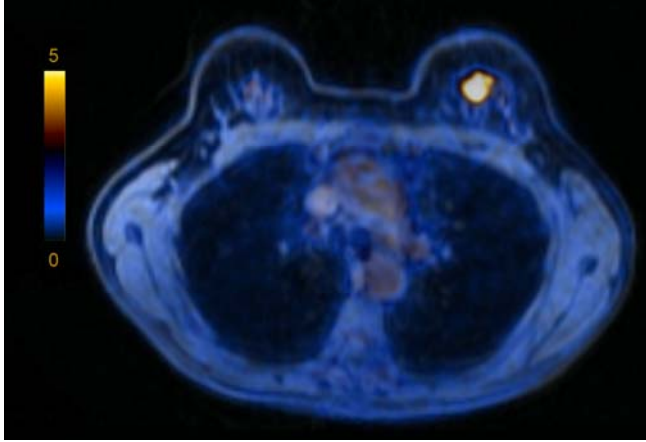
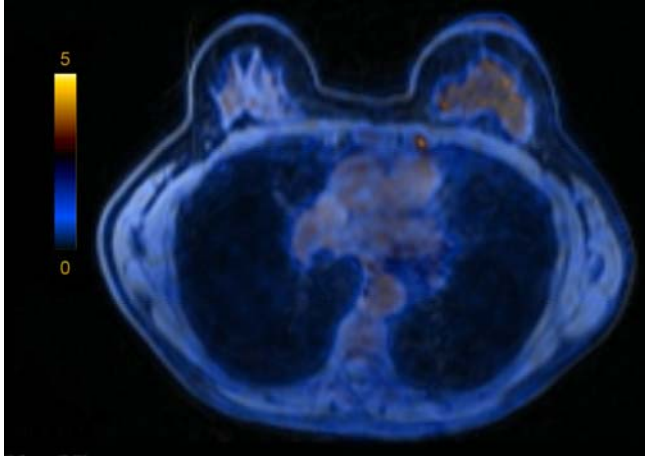**Figure 1** F: Axial fused PET/MRI image of the primary (PET with 10% dose).

Figure 1 G: Axial fused PET/MRI image of an internal mammary lymph node (PET with 10% dose).

TABLES

Table 1. Image Grading.

Category	General Image Quality + Artifact	Image Sharpness	Noise	Lesion Detectability
1	Excellent, no artifacts	Clear, excellent images	Negligible	Excellent
2	Good, some diagnostically irrelevant artifacts	Diagnostically irrelevant image blurring	Diagnostically irrelevant	Good
3	Average, diagnostically relevant artifacts	Diagnostically relevant image blurring	Diagnostically relevant	Average
4	Inadequate, marked artifacts	Inadequate image with blurring	Marked	Poor

Table 2. Results of Different Categories of Image Quality Assessment. Means +/- standard deviations (SD). Lesion detectability as a mean of all 71 lesions.

	General Image Quality + Artifacts		Image sharpness		Noise		Lesion detectability	
	mean	SD	mean	SD	mean	SD	mean	SD
2min	1.84	0.6	2.28	0.6	2.16	0.6	1.46	0.7
20min 100%	1.08	0.4	1.12	0.3	1.04	0.2	1.03	0.2
20min 20%	1.32	0.6	1.64	0.7	1.44	0.5	1.14	0.4
20min 10%	1.40	0.6	1.76	0.7	1.48	0.6	1.28	0.6
20min 5%	1.88	0.5	2.60	0.8	2.28	0.5	1.62	0.8

Table 3. Results of Comparison of means for different Reconstructions and Categories (Wilcoxon testing): GIQ+A, IS, noise, and LD.

p-value	General Image Quality + Artifacts	Image sharpness	Noise	Lesion detectability Primary Lesion	Lesion detectability Lymph Nodes
	2min	2min	2min	2min	2min
20min 100%	**<0.001**	**<0.001**	**<0.001**	**0.038**	**0.001**
20min 20%	**<0.001**	**<0.001**	**<0.001**	0.257	**0.001**
20min 10%	**0.001**	**0.001**	**0.001**	0.763	**0.032**
20min 5%	0.317	**0.005**	0.180	0.142	0.593

Supplemental Table 1. Technical Acquisition Parameters of MRI pulse sequences (IVIM sequence not counted for clinical acquisition time)

Sequences	Time (min)	FOV (cm)	Slice Thickness	TR (ms)	Bandwidth	TE (ms)	Flip Angle	Matrix Size
IVIM	05:20	36	5.0	8000	250	Minimum		160x160
ax VIBRANT dynamic	06:59	35.2	2.2	7.7	83.33	4.3	10	288x256
ax T2 STIR ASSET	04:06	36	4.0	7235	83.33	50	111	256x256
cor T2 FSE	03:13	34	4.0	3701	50.00	102.0	111	320x224
3D ax T1 ISO HR VIBRANT	02:11	35.2	1.0	5.0	62.50	2.3	10	352x352

Supplemental Table 2. Clinical Stage of Patients

T - category	-	10 x T1	15 xT2	1 x T3
N - category	18 x N0	3 x N1	4 x N2	1 x N3
M - category	23 x M0	3 x M1	-	-